

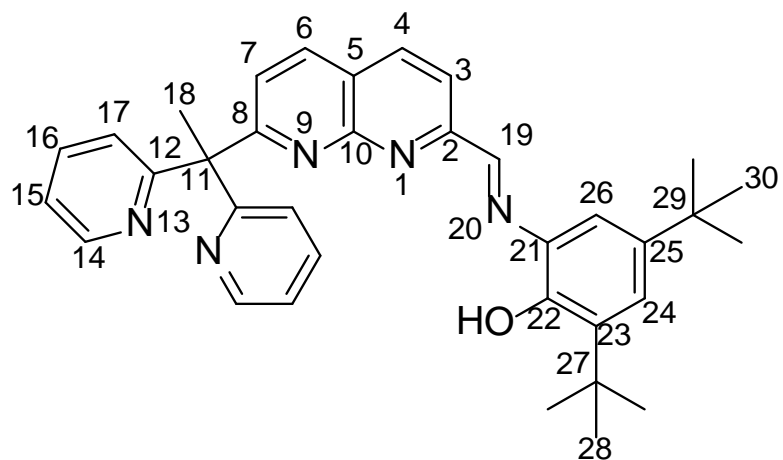
Supporting Information

Synthesis of unsymmetrical 1,8-naphthyridine-based ligands for assembly of tri- and tetra-nuclear copper(II) complexes

Felix Bacher, James A. Isaac, Christian Philouze, David Flot, Aurore Thibon-Pourret, and Catherine Belle

Contents:

Scheme S1. NMR numbering scheme for ligands, exemplified with HL^2 .	2
Figure S1. Part of the FT-IR spectra of $1^{tox} \cdot 2DMF$, $1^{tox} \cdot 2CH_3CN$, and H_2L^{1ox} .	3
Figure S2. ESI-MS of isolated complex $1^{tox} \cdot 2CH_3CN$ in acetonitrile solution.	4
Figure S3. A: Experimental (top) and theoretical (bottom) isotopic pattern for $[2M-CF_3SO_3]^+$ where $M = [Cu_2(L^{1ox})(\mu-OH)](CF_3SO_3)$, and B: Experimental (top) and theoretical (bottom) isotopic pattern for $[M-CF_3SO_3]^+$.	5
Figure S4. ORTEP view showing the combination of forms a and b in $[Cu_3(L^{2ox})_2(\mu-OH)_2] \cdot H_2O$ ($2^{triox} \cdot H_2O$).	6
Figure S5. ESI-MS data of $2^{triox} \cdot H_2O$ in acetonitrile: experimental (top) and simulated (down) isotopic pattern for the monocharged peak at 718.2 corresponding to $[Cu_2L^{2ox})(OH)_2] + H^+$ ($[(C_{35}H_{35}N_5O_2)(OH)_2] + H^+$).	7
Figure S6: 1H NMR spectrum of HL^1 in $DMSO-d_6$ (500 MHz).	8
Figure S7: ^{13}C NMR spectrum of HL^1 in $DMSO-d_6$ (126 MHz).	9
Figure S8: 1H NMR spectrum of HL^2 in $DMSO-d_6$ (500 MHz).	10
Figure S9: ^{13}C NMR spectrum of HL^2 in $DMSO-d_6$ (126 MHz).	11
Figure S10: 1H NMR spectrum of H_2L^{1ox} in $DMSO-d_6$ (500 MHz).	12
Figure S11: ^{13}C NMR spectrum of H_2L^{1ox} in $DMSO-d_6$ (126 MHz).	13
Figure S12: 1H NMR spectrum of H_2L^{2ox} in $DMSO-d_6$ (500 MHz).	14
Figure S13: ^{13}C NMR spectrum of H_2L^{2ox} in $DMSO-d_6$ (126 MHz).	15
Table S1. Selected bond lengths (Å) and angles (°) for $[Cu_4(L^{1ox})_2(\mu-OH)_2](CF_3SO_3)_2 \cdot 2DMF$ ($1^{tox} \cdot 2DMF$).	16



Scheme S1. NMR numbering scheme for ligands, exemplified with HL².

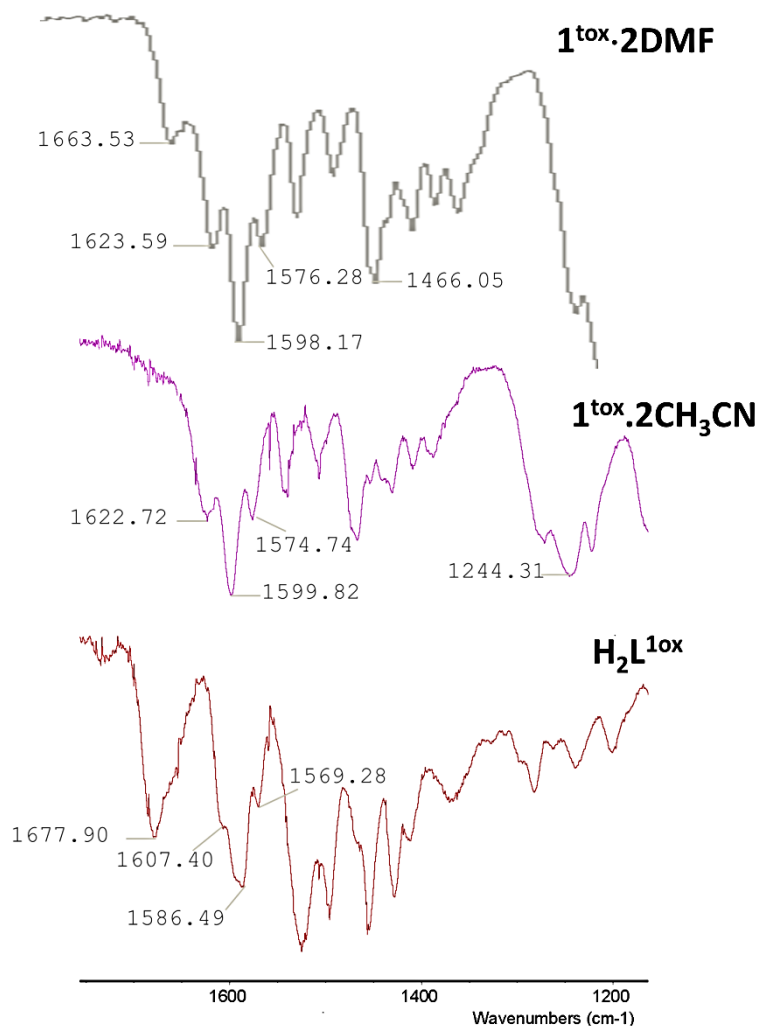


Figure S1. Part of the FT-IR spectra of **1^{tox}·2DMF**, **1^{tox}·2CH₃CN**, and **H₂L^{1ox}**

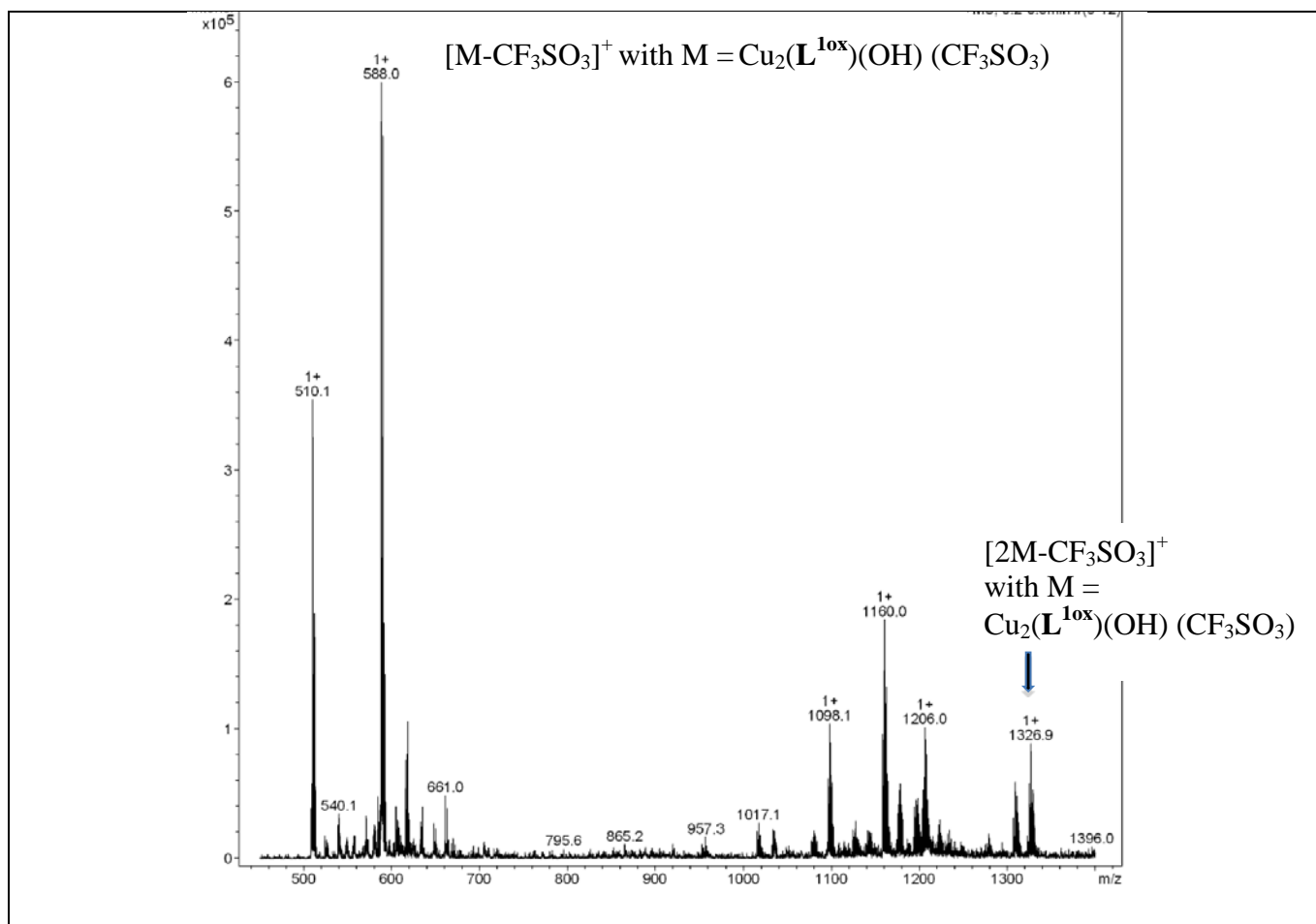


Figure S2. ESI-MS of isolated complex $1^{tox} \cdot 2CH_3CN$ in acetonitrile solution.

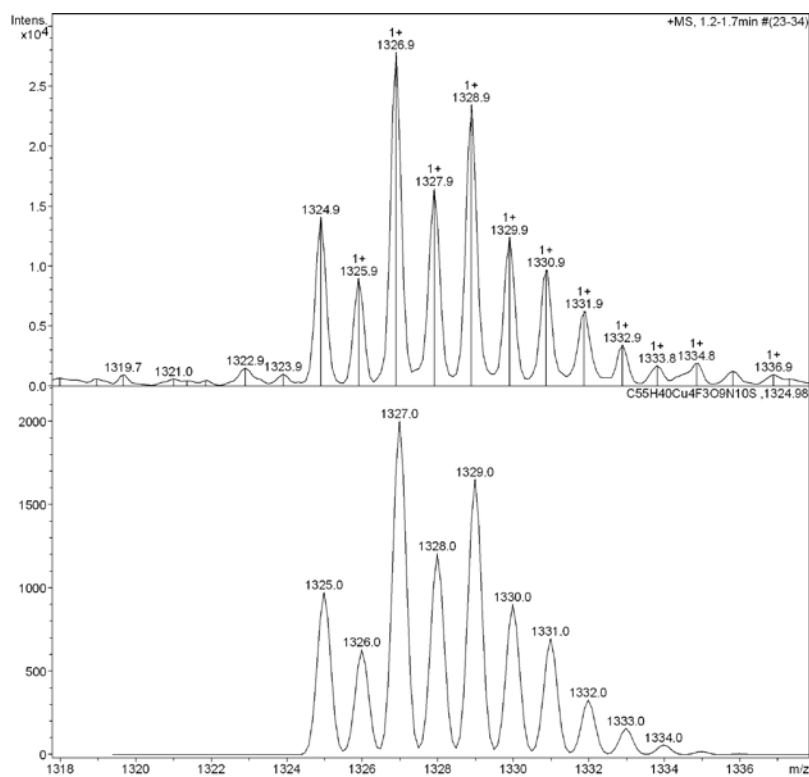
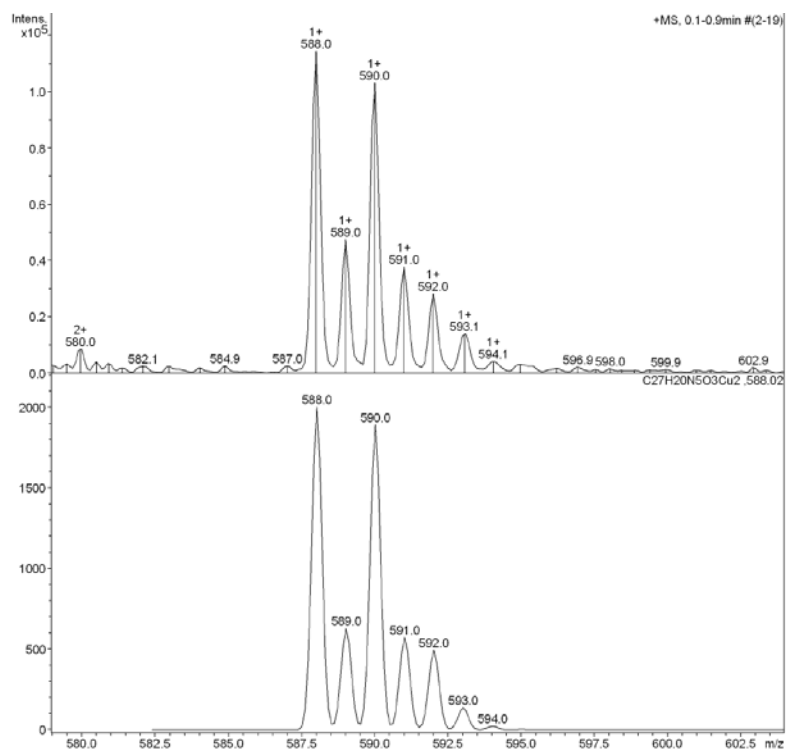
A**B**

Figure S3. **A**: Experimental (top) and theoretical (bottom) isotopic pattern for $[2M-CF_3SO_3]^+$ where $M = [Cu_2(L^{1ox})(\mu-OH)](CF_3SO_3)$, and **B**: Experimental (top) and theoretical (bottom) isotopic pattern for $[M-CF_3SO_3]^+$

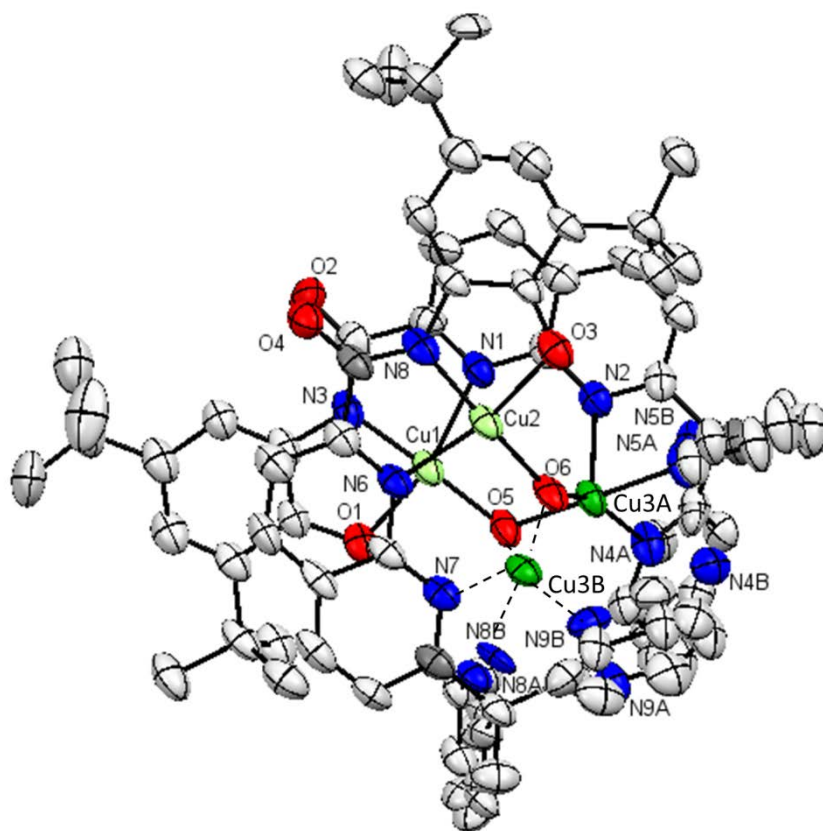


Figure S4. ORTEP view showing the combination of forms **a** and **b** in $[\text{Cu}_3(\text{L}^{2\text{ox}})_2(\mu\text{-OH})_2]\cdot\text{H}_2\text{O}$ ($2^{\text{triox}}\cdot\text{H}_2\text{O}$). Hydrogen atoms and H_2O molecule were removed for clarity. Color code; red: oxygen, blue: nitrogen, copper: green with Cu3 (two forms) in dark green. Plot of coordination bonds around Cu3 in form **b** (Cu3B) is represented in dashed lines.

Selected bond lengths (Å) and angles (°) related to Cu3 in form **b**: Cu1...Cu3B 3.097, Cu2...Cu3B 3.248, Cu3B-O5 1.749(7), Cu3B-N9B 2.030(19), Cu3B-N8B 1.94(3), Cu3B-O6 1.884(6); Cu2 O6 Cu3B 119.6(3), Cu1 O5 Cu3B 117.3(3), O6 Cu3B O5 100.1(3), O6 Cu3B N7 87.5(3), O6 Cu3B N8B 171.1(10), O6 Cu3B N9B 82.5(7), O5 Cu3B N7 123.5(3), O5 Cu3B N8B 88.7(10), O5 Cu3B N9B 152.2(8), N8B Cu3B N7 86.3(9), N9B Cu3B N7 85.2(8), N8B Cu3B N9B 90.6(13).

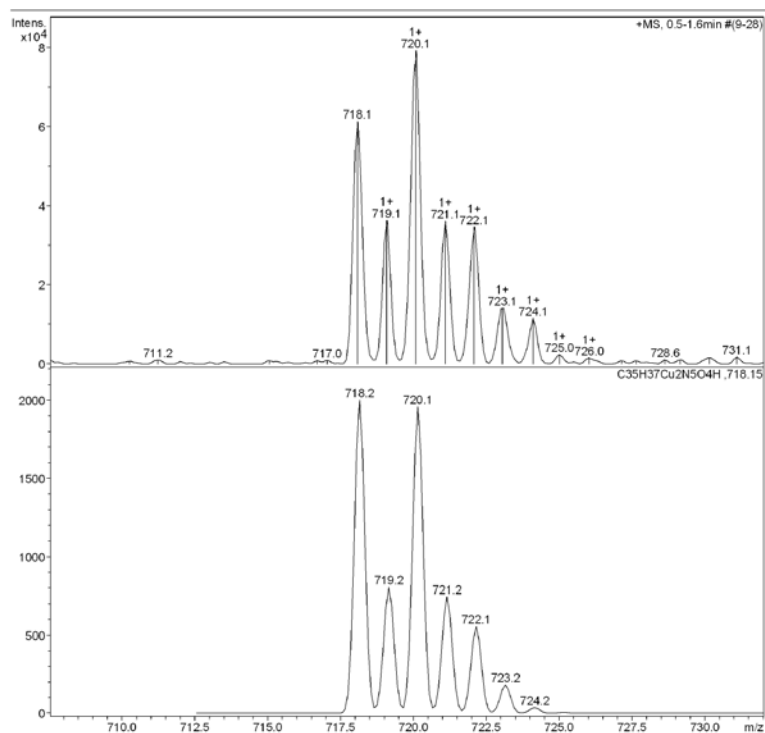


Figure S5. ESI-MS data of $2^{\text{triox}} \cdot \text{H}_2\text{O}$ in acetonitrile: experimental (top) and simulated (down) isotopic pattern for the monocharged peak at 718.2 corresponding to $[\text{Cu}_2\text{L}^{2\text{ox}}](\text{OH})_2 + \text{H}^+$ ($[(\text{C}_{35}\text{H}_{35}\text{N}_5\text{O}_2)(\text{OH})_2] + \text{H}^+$)

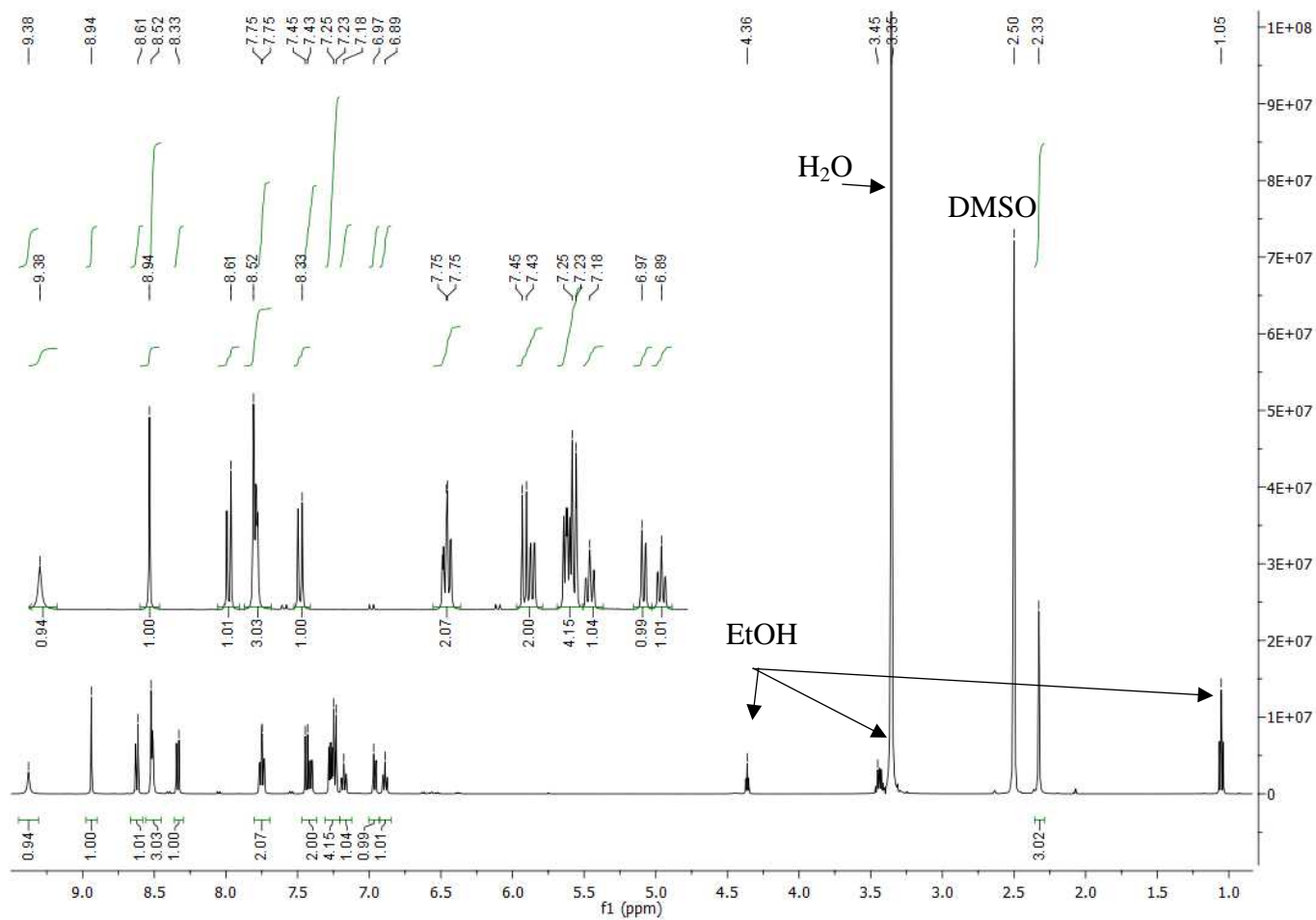
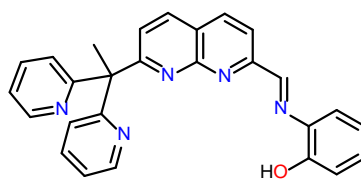


Figure S6: ¹H NMR spectrum of HL¹ in DMSO-*d*₆ (500 MHz).

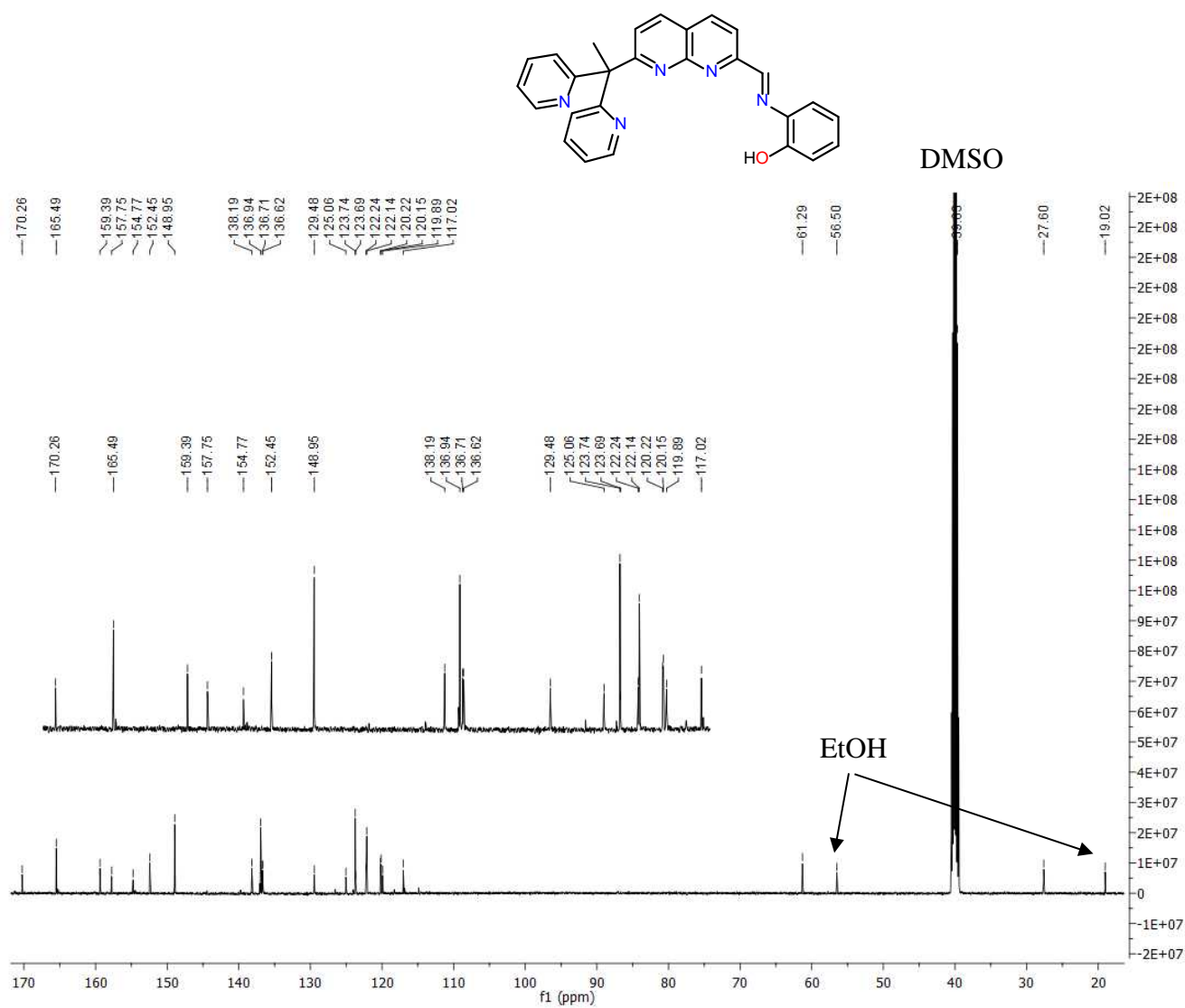


Figure S7: ¹³C NMR spectrum of HL¹ in DMSO-*d*₆ (126 MHz).

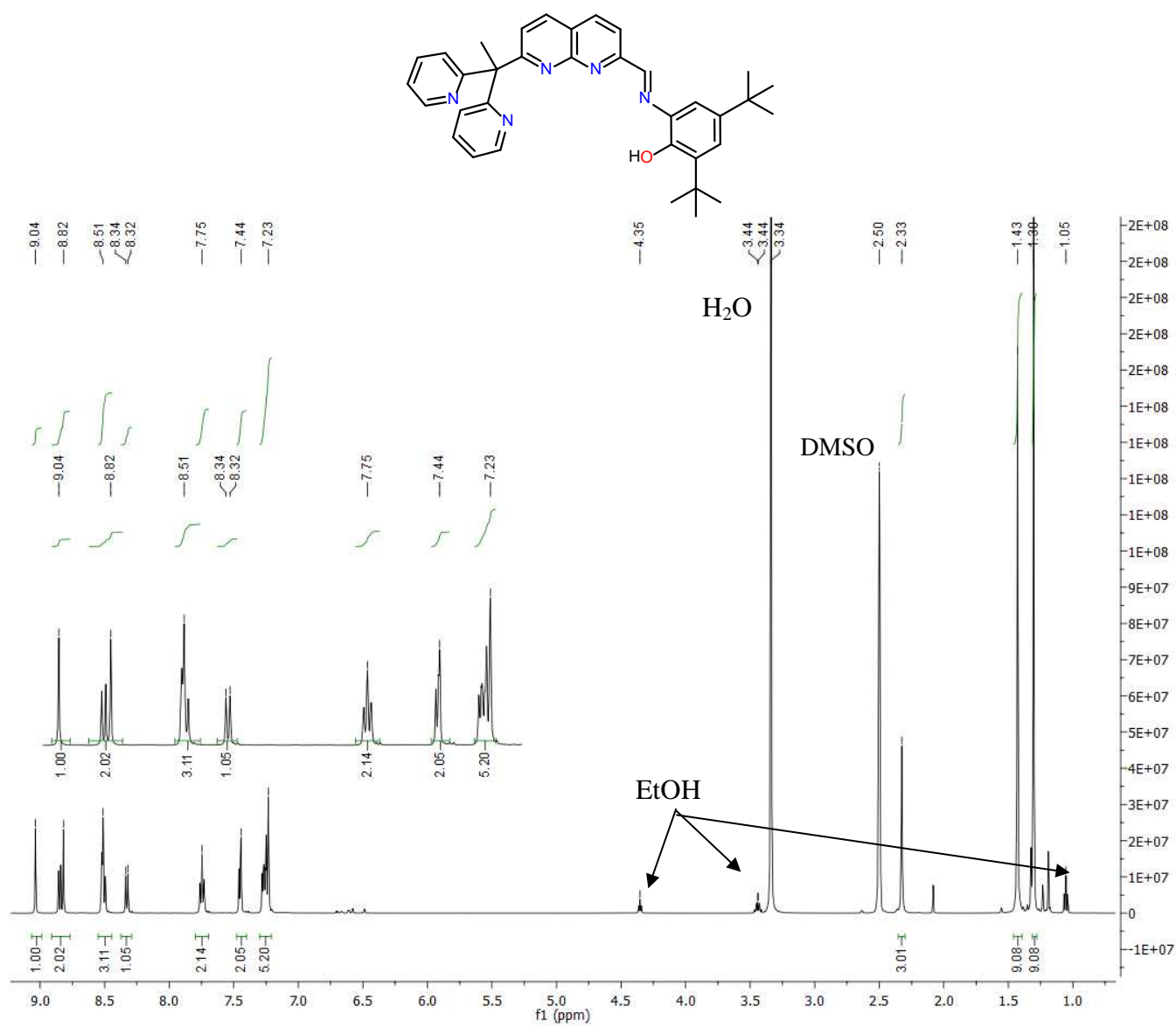


Figure S8: ¹H NMR spectrum of **HL²** in DMSO-*d*₆ (500 MHz).

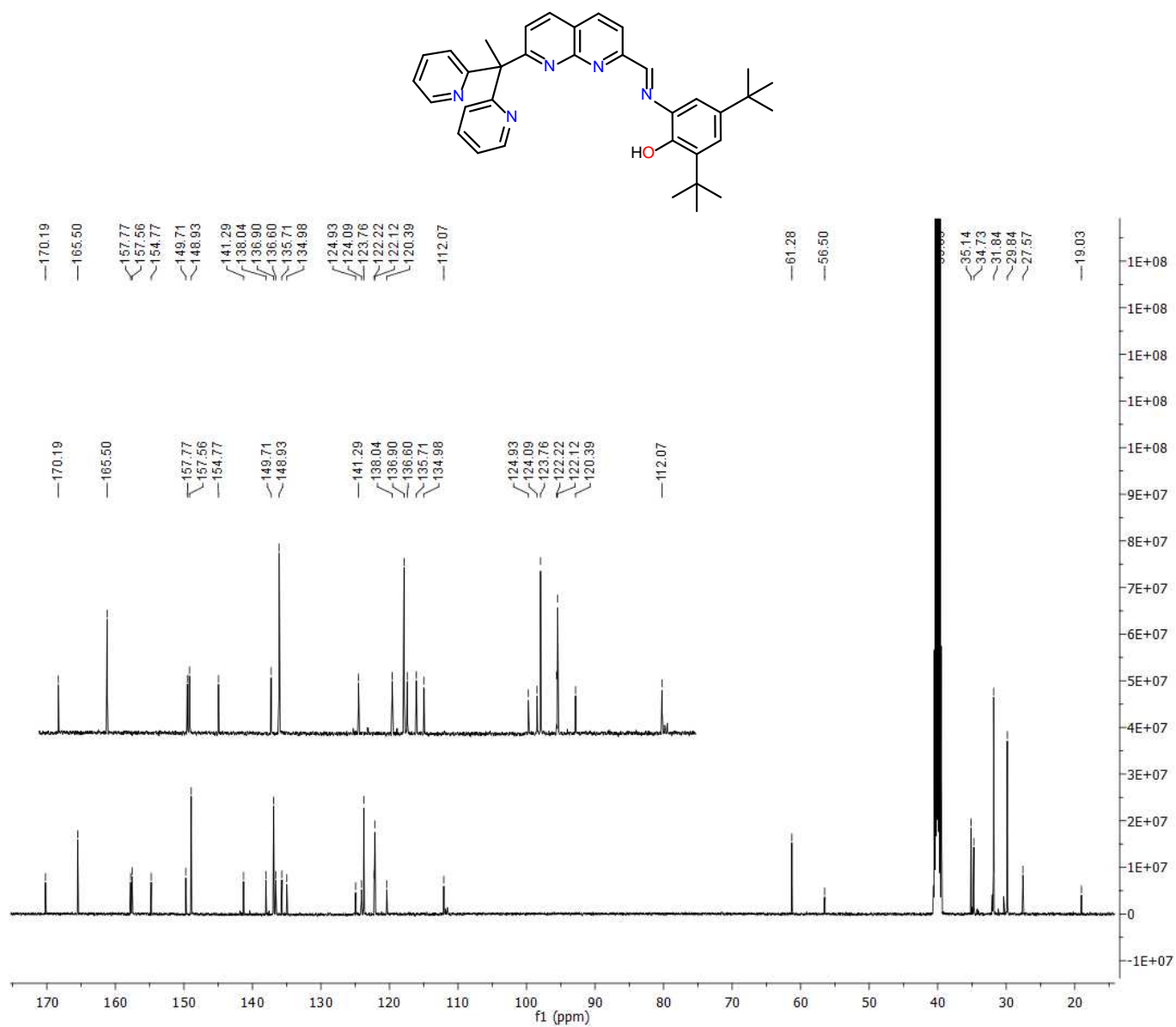


Figure S9: ¹³C NMR spectrum of HL² in DMSO-*d*₆ (126 MHz).

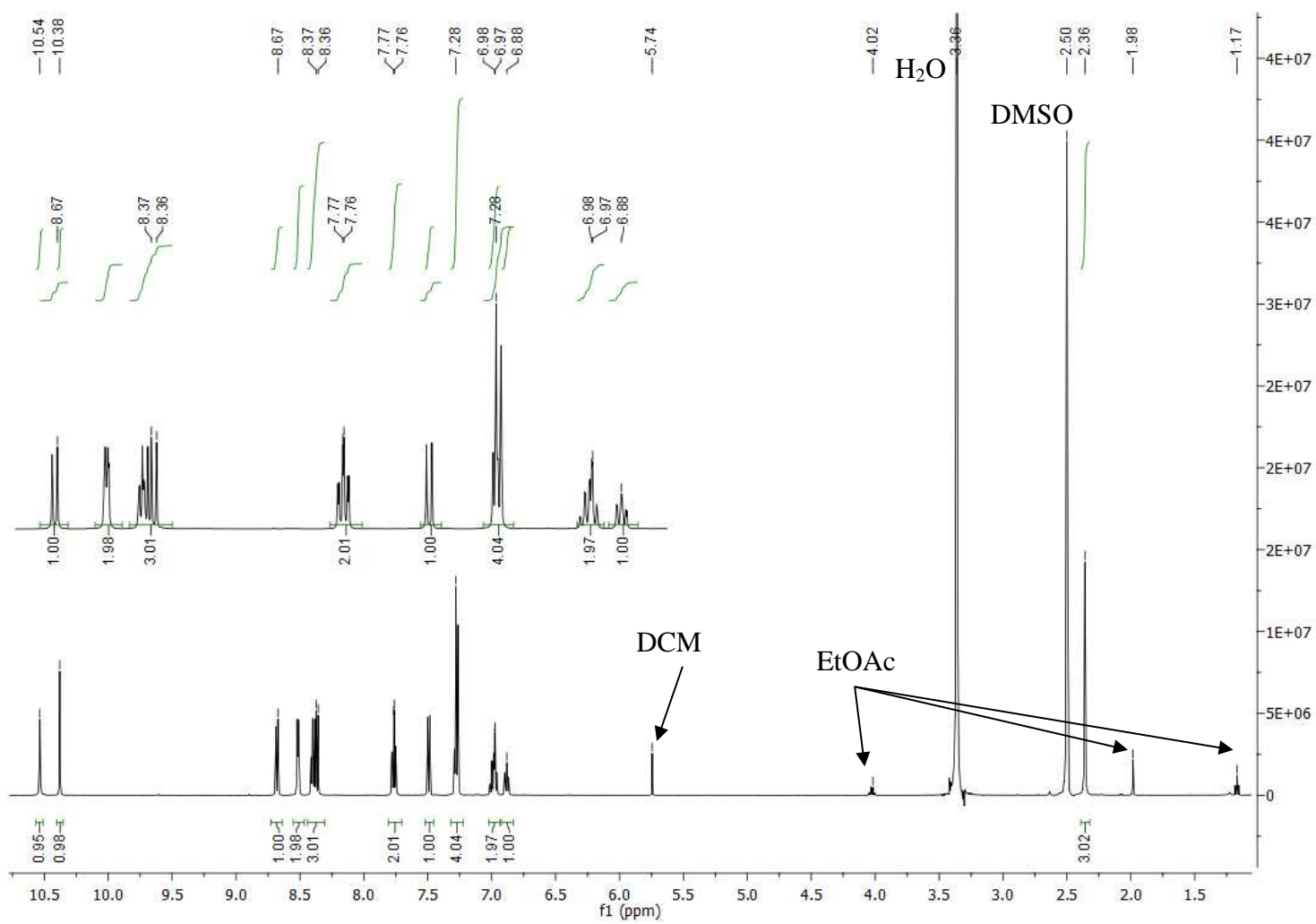
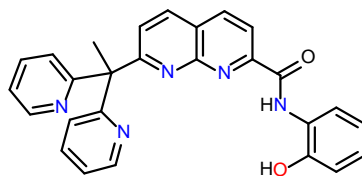


Figure S10: 1H NMR spectrum of H_2L^{10x} in $DMSO-d_6$ (500 MHz).

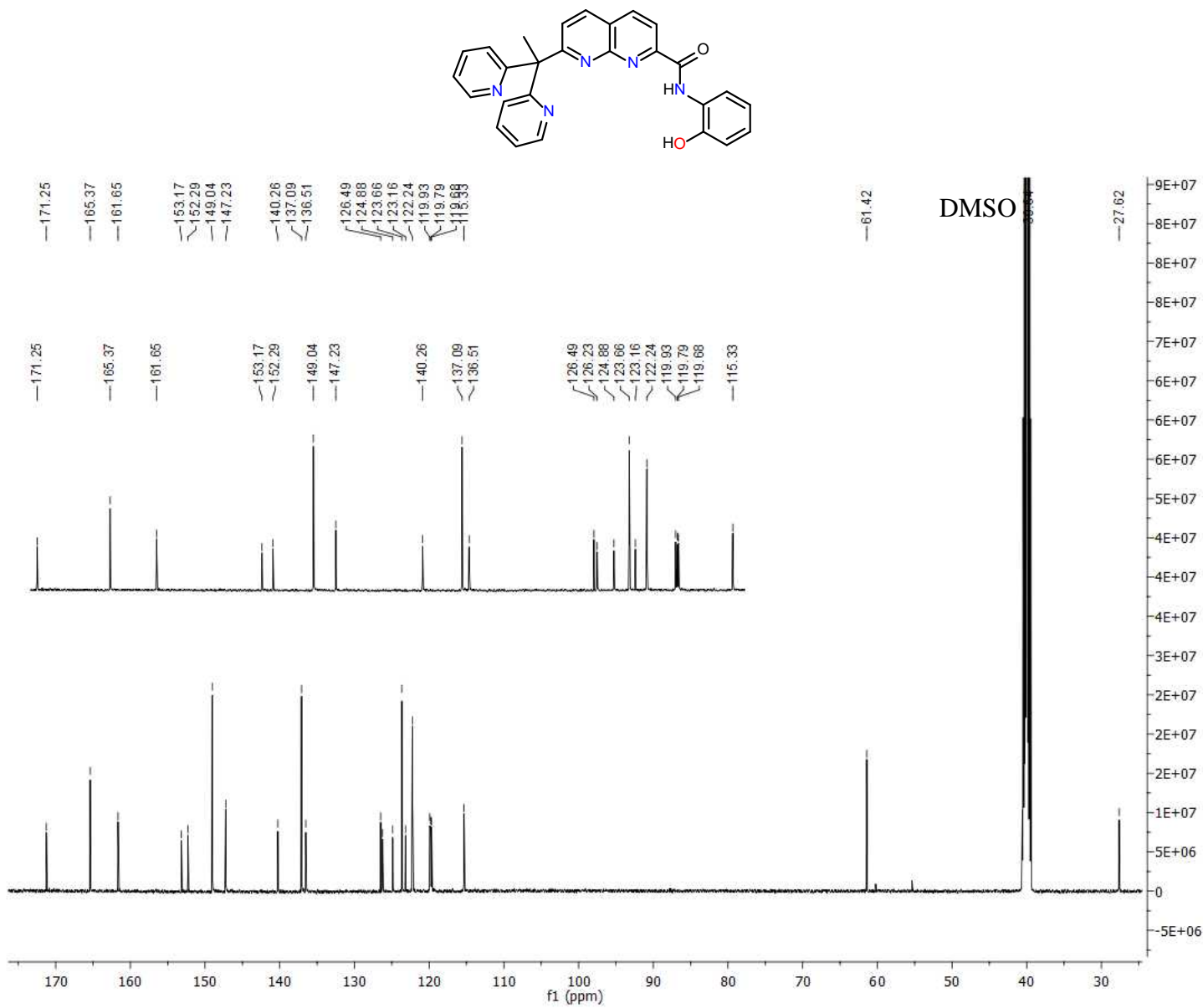


Figure S11: ^{13}C NMR spectrum of H_2L^{1ox} in $DMSO-d_6$ (126 MHz).

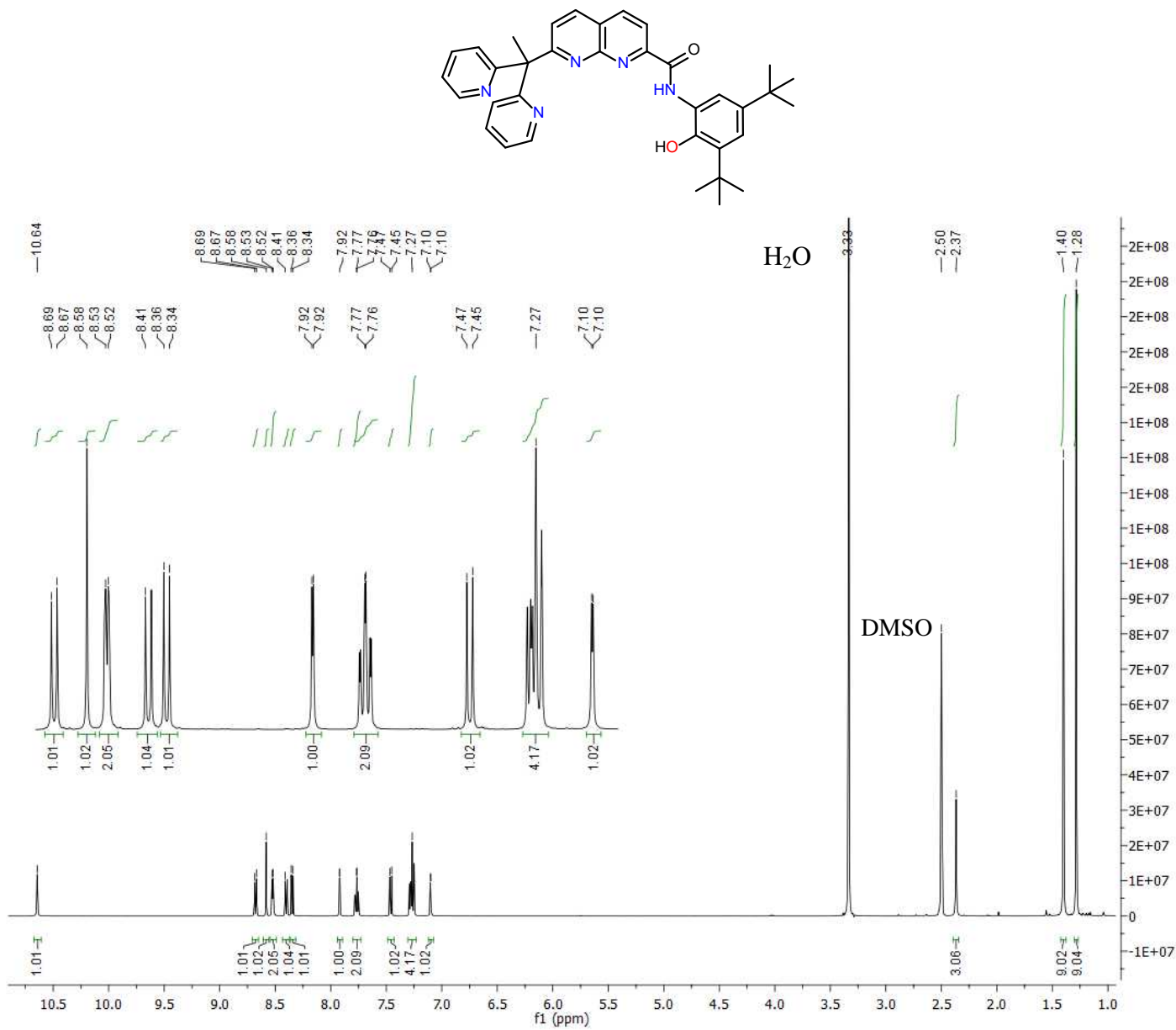


Figure S12: 1H NMR spectrum of H_2L^{20x} in $DMSO-d_6$ (500 MHz).

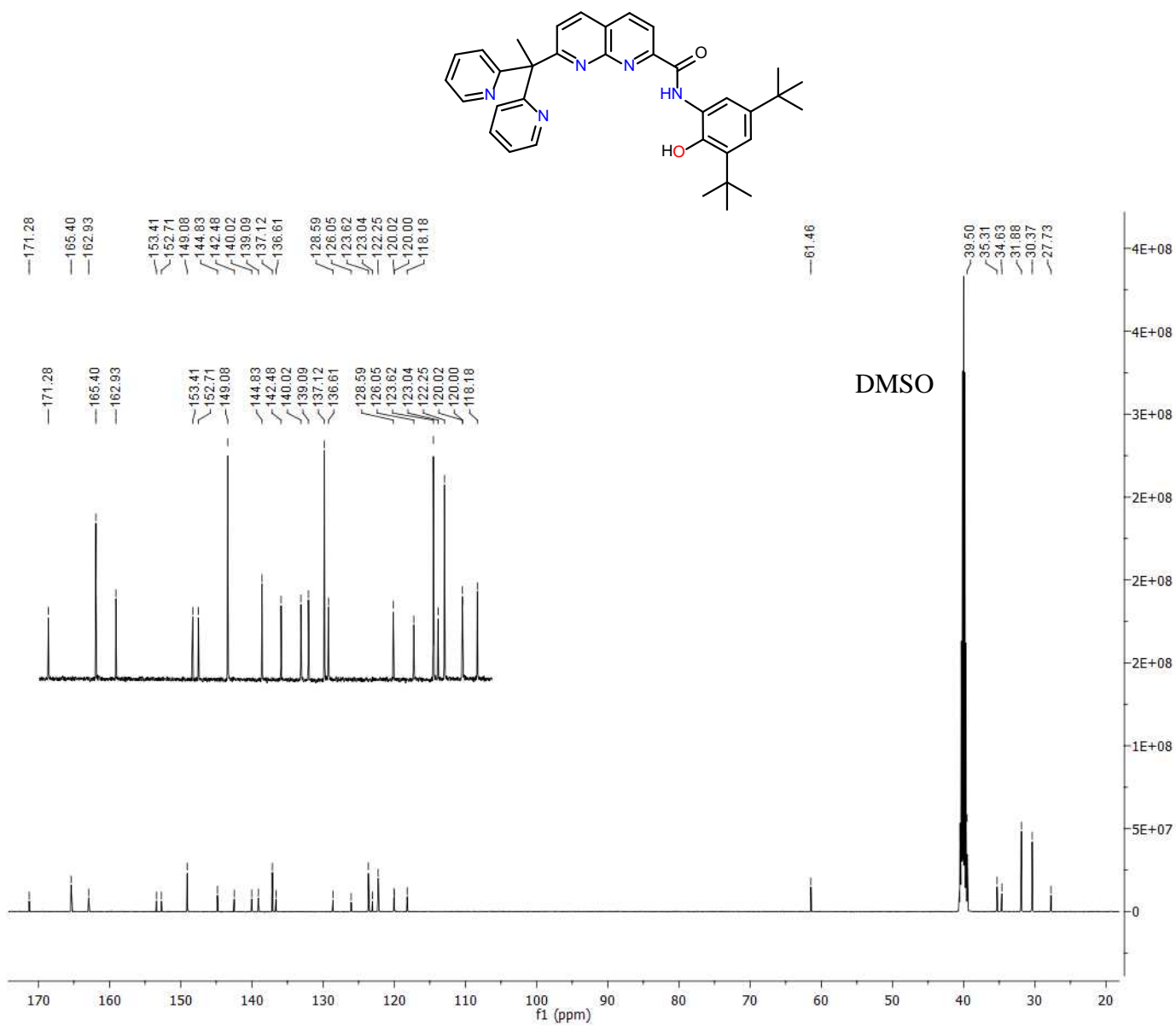


Figure S13: ^{13}C NMR spectrum of H_2L^{20x} in $DMSO-d_6$ (126 MHz).

Table S1. Selected bond lengths (Å) and angles (°) for [Cu₄(L^{1ox})₂(μ-OH)₂](CF₃SO₃)₂·2DMF (1^{1ox}·2DMF)

Selected distances (Å)		Selected angles (°)	
Cu1...Cu2	2.9637(8)	Cu1 O1 Cu2'	118.56(13)
Cu1...Cu2'	3.453	O1 Cu1 N1	165.47(13)
Cu1...Cu1'	3.135	O3 Cu1 O1	89.67(12)
Cu2...Cu2'	4.142	O3 Cu1 N1	103.74(13)
Cu1 O1'	2.642	O3 Cu1 N3	173.73(14)
Cu1 O1	1.979(3)	N3 Cu1 O1	84.07(14)
Cu1 O3	1.892(3)	N3 Cu1 N1	82.52(15)
Cu1 N1	2.069(3)	Cu1 O3 Cu2	102.21(13)
Cu1 N3	1.889(3)	O1 Cu2 N2	99.51(12)
Cu2 O1	2.038(3)	O3 Cu2 O1	92.39(12)
Cu2 O3	1.916(3)	O3 Cu2 N2	99.51(12)
Cu2 N2	2.226(3)	O3 Cu2 N4	171.36(14)
Cu2 N4	1.972(4)	O3 Cu2 N5	90.74(13)
Cu2 N5	2.018(3)	N4 Cu2 O1	90.29(13)
		N4 Cu2 N2	91.28(15)
		N4 Cu2 N5	85.79(15)
		N5 Cu2 O1	173.40(13)
		N5 Cu2 N2	85.91(14)